

Thermodynamics on formation of C, Al_4C_3 and Al_2O_3 in AlCl disproportionation process in vacuum to produce aluminum

Yue-bin FENG¹, Bin YANG², Yong-nian DAI²

1. Faculty of Science, Kunming University of Science and Technology, Kunming 650500, China;
2. National Engineering Laboratory of Vacuum Metallurgy, Faculty of Metallurgy and Energy Engineering, Kunming University of Science and Technology, Kunming 650093, China

Received 11 November 2013; accepted 21 March 2014

Abstract: The formation conditions of C, Al_4C_3 and Al_2O_3 in the AlCl disproportionation process in vacuum to produce aluminum was investigated by thermodynamics analysis. It is demonstrated that the required temperatures for the reactions to form these impurities, the disproportionation of CO and the reactions of metallic aluminum with CO, decrease with decreasing pressure. The $\lg p_{\text{CO}} - 1/T$ diagram of metallic aluminum–CO system agrees with the experimental results, indicating that the reaction rate is very high and this system in vacuum is approximately in equilibrium; therefore, the equilibrium diagram can be used to predict the possible reactions in this system in vacuum.

Key words: Al; AlCl ; Al_2O_3 ; Al_4C_3 ; disproportionation; vacuum

1 Introduction

The traditional Hall–Héroult process is the major industrial process for the production of aluminum today, characterized by high energy consumption and high cost. The carbothermal reduction process is a promising alternative to cut cost [1,2]; however, it requires high temperatures of 2300–2500 K [3–5], at which the aluminum product, byproducts and unreacted raw materials melt, and it is difficult to separate aluminum from the melt [4–6]. The AlCl disproportionation process was developed from the direct carbothermal process; its required temperatures are below 2073 K; and the aluminum product is apart from the raw materials [7,8].

The AlCl disproportionation process in vacuum can proceed at a much lower temperature [9,10]. And some research on it has been carried out, involving mechanism [11–13], behaviors of impurities in raw materials [14–15], and extraction conditions of aluminum [10]. The purity of aluminum is not satisfactory for the metallic aluminum can absorb CO to catalyze its disproportionation to C and CO_2 , and react with CO to form Al_4C_3 , Al_2O_3 , C and CO_2 , resulting in aluminum products containing Al_4C_3 , Al_2O_3 and C [12].

Gibbs free energy change is often used to predict the thermodynamic feasibility of a chemical reaction, and it is also suitable for the reactions in vacuum [16]. Thermodynamic equilibrium diagram can be used to determine the existence area of various species in a reaction system; however, it hardly ever was used for the reaction systems in vacuum. It is speculated that the existence area of various species for a system in vacuum will deviate from the equilibrium diagram constructed by thermodynamic calculations because it is in non-equilibrium state. However, the higher the reaction rate, the smaller the deviation, and hence the thermodynamic equilibrium diagram could be also useful for some of the reaction systems in vacuum.

This work is an attempt to investigate the formation conditions of Al_4C_3 , Al_2O_3 and C in the AlCl disproportionation process in vacuum to produce aluminum using Gibbs free energy change together with thermodynamic equilibrium diagram in order to provide some bases for control of these impurities in aluminum products.

2 Experimental

The experimental investigation on the AlCl

Foundation item: Project (51364020) supported by the National Natural Science Foundation of China

Corresponding author: Yue-bin FENG; Tel: +86-871-65916456; E-mail: fenjys@126.com

DOI: 10.1016/S1003-6326(14)63478-6

disproportionation process to produce aluminum was described in Ref. [12]. The vacuum furnace used in the experiments was described in detail in Refs. [12,17], as shown in Fig. 1. The temperature in the condenser is below 1200 K and decreases gradually from the bottom to the top. The top is next to the water-cooled cover of the furnace, so its temperature is very low.

The pellets made of alumina and graphite in the crucible reacted with gaseous AlCl_3 to form gaseous AlCl and CO at high temperatures. As the gases along with unreacted AlCl_3 went through the condenser, the condensates formed with decreasing temperature. The condensates consisted of Al, Al_4C_3 , Al_2O_3 and C [12]. The metallic aluminum as product was formed from the disproportionation of AlCl , and the Al_4C_3 , Al_2O_3 and C as impurities were formed from the disproportionation of CO and the reactions of metallic aluminum with CO [12].

The pressure determined at the exit of the vacuum furnace was maintained at 5–200 Pa in the experimental process [12]. Additionally, the off gases were analyzed by the gas chromatograph in this work, containing about 1.5% CO_2 and about 98.5% CO.

3 Thermodynamics analysis

3.1 Disproportionation of CO

CO can disproportionate into C and CO_2 with decreasing temperature when it is absorbed on metallic catalysts. Metallic aluminum should act as a catalyst in the AlCl disproportionation process.

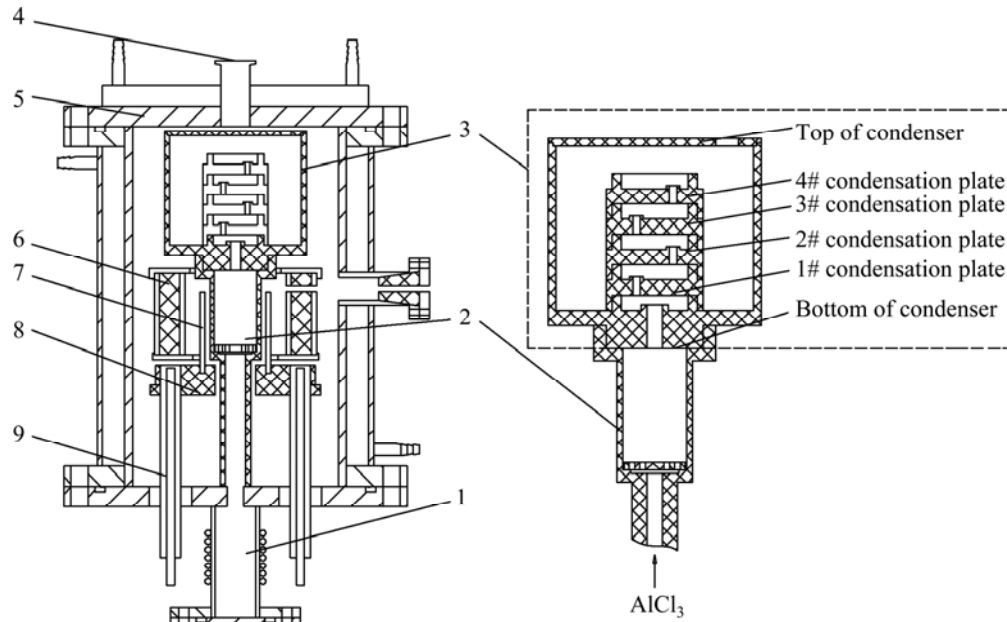


Fig. 1 Schematic diagram of vacuum furnace [12]: 1— AlCl_3 evaporator; 2—Reaction crucible; 3—Graphite condenser; 4—Exit connected with vacuum pump; 5—Water-cooled cover of furnace; 6—Thermal insulating layer; 7—Graphite exothermic body; 8—Exothermic body base; 9—Water-cooled electrode

Based on the data of Thermochemical Calculation Software HSC, the standard Gibbs free energy changes (ΔG^\ominus) of Reaction (1) in the range of 300–1900 K were calculated as shown in Fig. 2. As can be seen, ΔG^\ominus increases with increasing temperature (T). The correlation coefficient (r) between ΔG^\ominus and T was calculated to be 0.9999. The regression equation is shown as Eq. (2).

$$\Delta G^\ominus = -170598 + 174.35T \quad (2)$$

From Eq. (2), ΔG^\ominus equals zero when T is 978 K. This is to say that the disproportionation of CO is thermodynamically possible at temperatures lower than 978 K in the standard atmosphere.

In the nonstandard atmosphere, the Gibbs free energy change (ΔG) of Reaction (1) is a function of temperature (T) and pressure (p), shown as Eq.(3), which is deduced from Eq. (1) and Eq. (2).

$$\Delta G = -170598 + 174.4T + 19.146T \lg \left[\frac{p_{\text{CO}_2}/p^\ominus}{(p_{\text{CO}}/p^\ominus)^2} \right] \quad (3)$$

Equation (4) is obtained from Reaction (1), where α is the disproportionation rate of CO.

$$p_{\text{CO}_2} = p_{\text{CO}}(\alpha/2)/(1-\alpha) \quad (4)$$

The total pressure p_{tot} is set to equal the sum of partial pressures of CO and CO_2 , and consequently the relationship between p_{tot} and p_{CO} can be expressed as Eq. (5).

$$p_{\text{tot}} = p_{\text{CO}} + p_{\text{CO}}(\alpha/2)/(1-\alpha) \quad (5)$$

The off gas in the experiment consisted of about 1.5% CO_2 and about 98.5% CO. The CO was generated

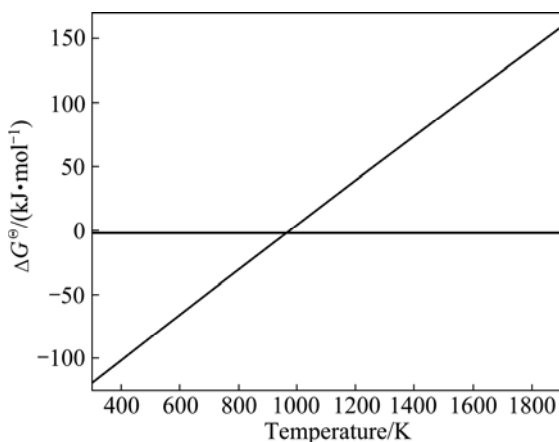


Fig. 2 ΔG^\ominus of Reaction (1) vs temperature

from the carbothermal reduction–chlorination of alumina, and the CO_2 mainly from the disproportionation of CO. From this, α was about 1.5%. In fact, as the CO passed through the condenser, it could react with metallic aluminum, resulting in some increase in CO_2 and some decrease in CO, and thereby α should be below 1.5%.

When α was 1.5%, ΔG at different pressures in the range of 300–1900 K were calculated from Eqs. (3)–(5), as shown in Fig. 3. As can be seen, the required temperature for the disproportionation of CO decreases with decreasing total pressure. When the total pressures are 200, 100 and 5 Pa, the equilibrium temperatures are 917, 890 and 787 K, respectively.

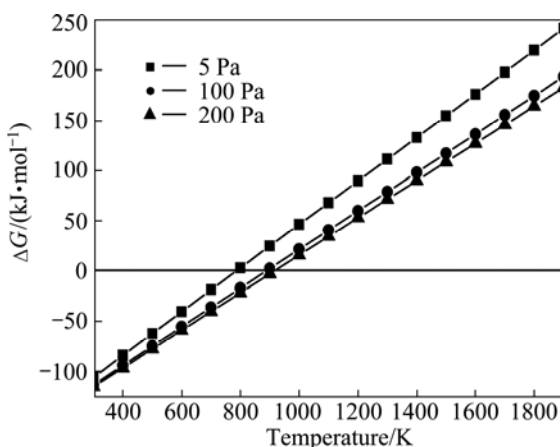
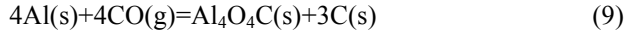
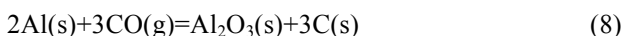
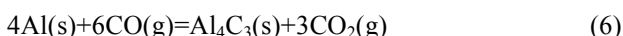


Fig. 3 ΔG of Reaction (1) vs temperature at reduced pressures ($\alpha=1.5\%$)

3.2 Reactions between metallic aluminum and CO

The possible reactions between metallic aluminum and CO are shown as follows:



3.2.1 Gibbs free energy changes of reactions between metallic aluminum and CO

Based on the data of HSC, ΔG^\ominus of each possible reaction between metallic aluminum and CO in the range of 300–1900 K was calculated as shown in Fig. 4. A very nice linear relation can be found between ΔG^\ominus of Reactions (6) to (10) and T , and the regression equations are shown as Eqs. (11)–(15). ΔG^\ominus increases with increasing temperature, and they are all negative below 1233 K for Reaction (6) and in the range of 300–1900 K for Reactions (7)–(10).

$$\Delta G_6^\ominus = -740481 + 600.4T \quad (11)$$

$$\Delta G_7^\ominus = -1574111 + 663.7T \quad (12)$$

$$\Delta G_8^\ominus = -1345994 + 587.4T \quad (13)$$

$$\Delta G_9^\ominus = -1878850 + 793.5T \quad (14)$$

$$\Delta G_{10}^\ominus = -2106967 + 870.3T \quad (15)$$

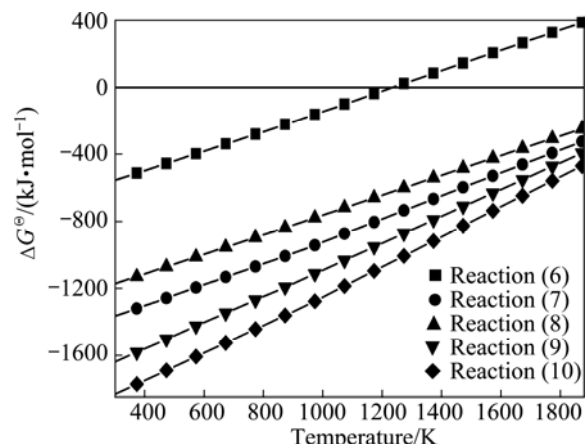


Fig. 4 ΔG^\ominus of Reactions (6) to (10) vs temperature

In the nonstandard atmosphere, the Gibbs free energy change (ΔG) is a function of T and p .

For Reaction (6), ΔG is defined as Eq. (16).

$$\Delta G = \Delta G^\ominus + RT \ln[(p_{\text{CO}_2}/p^\ominus)^3 / (p_{\text{CO}}/p^\ominus)^6] \quad (16)$$

Without considering the differences in the pressures of CO and CO_2 between the condenser and the exit, the partial pressure of CO in the condenser equaled approximately the total pressure of CO and CO_2 , $p_{\text{CO}} \approx p_{\text{tot}}$, and the partial pressure of CO_2 equaled approximately 0.015 times the total pressure, $p_{\text{CO}_2} \approx 0.015 p_{\text{tot}}$, due to the off gases consisting of about 1.5% CO_2 and about 98.5% CO. Substituting them and Eq. (11) into Eq. (16), ΔG as a function of T and p_{tot} can be expressed as Eq. (17).

$$\Delta G_6 = -740481 + 782.79T - 57.44T \lg p_{\text{tot}} \quad (17)$$

In the same way, ΔG values of Reactions (7) to (10) as a function of T and p_{tot} can be deduced and expressed as Eqs. (18) to (21).

$$\Delta G_7 = -1574111 + 950.9T - 57.44T \lg p_{\text{tot}} \quad (18)$$

$$\Delta G_8 = -1345994 + 874.6T - 57.44T \lg p_{\text{tot}} \quad (19)$$

$$\Delta G_9 = -1878850 + 1176.4T - 76.58T \lg p_{\text{tot}} \quad (20)$$

$$\Delta G_{10} = -2106967 + 1253.2T - 76.58T \lg p_{\text{tot}} \quad (21)$$

From Eqs. (17)–(21), the ΔG – T curves at different total pressures for Reactions (6)–(10) were obtained as shown in Fig. 5. As can be seen, ΔG increases with

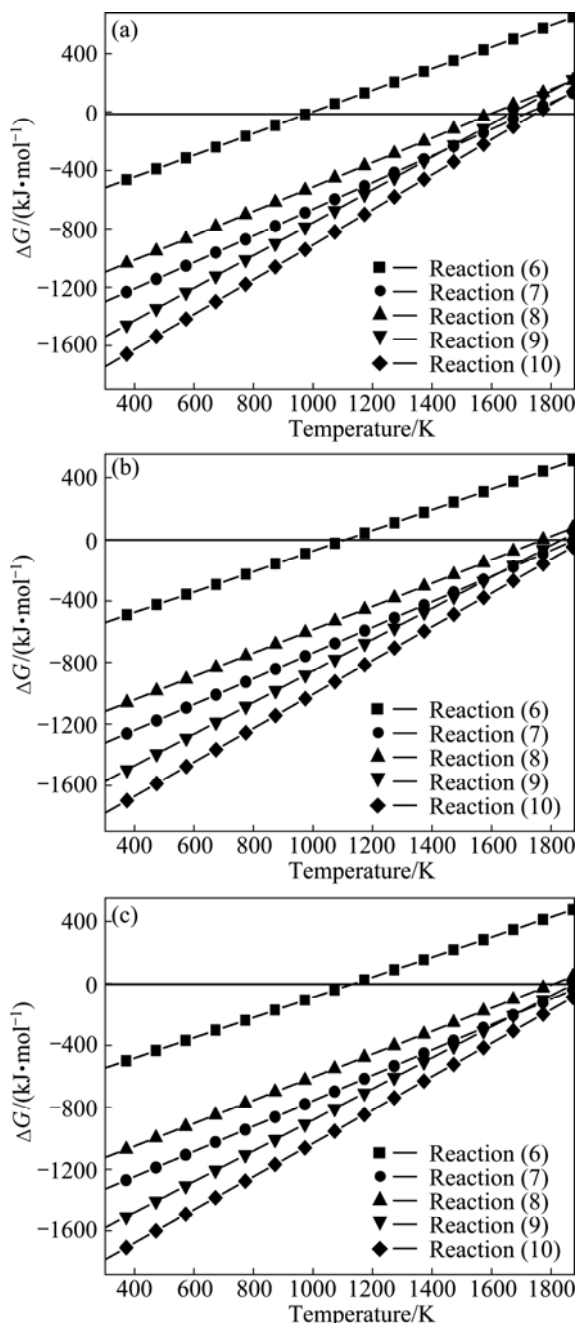


Fig. 5 ΔG of Reactions (6) to (10) vs temperature at reduced pressures: (a) 5 Pa; (b) 100 Pa; (c) 200 Pa

increasing temperature, and the onset temperatures decrease with decreasing total pressure. When the total pressure is 200 Pa, the onset temperature of Reactions (6), (8) and (9) are 1138, 1813 and 1878 K, respectively, and ΔG values of Reactions (7) and (10) are all negative below 1900 K. When the total pressure is 100 Pa, the onset temperatures of Reactions (6)–(9) are 1109, 1883, 1772 and 1836 K, respectively, and ΔG of Reaction (10) is negative below 1900 K. When the total pressure is 5 Pa, the onset temperatures of Reactions (6)–(10) are 997, 1728, 1613, 1673 and 1756 K, respectively. Accordingly, the required temperature from low to high is as follows: Reaction (6), Reaction (8), Reaction (9), Reaction (7) and Reaction (10).

3.2.2 Equilibrium diagram of metallic aluminum–CO reaction system

Providing that metallic aluminum reacts with CO according to one of Reactions (6)–(10), the equilibrium diagram of Al–CO system can be designed.

For Reaction (6), the number of degrees of freedom in the system is 2, $f=(4-1)-3+2=2$, and the factors affecting the equilibrium are temperature, partial pressure of CO_2 , and partial pressure of CO. When the partial pressure rate of CO_2 to CO is 0.015, the equilibrium is determined by temperature and partial pressure of CO, $p_{\text{CO}}=\varphi(T)$. By substituting $p_{\text{CO}_2} = 0.015 p_{\text{CO}}$ into Eq. (16), and setting ΔG to be zero, the relation between p_{CO} and T at equilibrium is obtained as shown in Eq. (22).

$$\lg p_{\text{CO}} = 11.93 - 9669.4/T \quad (22)$$

For Reactions (7) to (10), the number of degrees of freedom in the system is 1, $f=(4-1)-4+2=1$, and the factors affecting the equilibrium are temperature and pressure of CO, $p_{\text{CO}}=\varphi(T)$. By setting ΔG to be zero, the relations between p_{CO} and T at equilibrium are deduced as shown in Eqs. (23) to (26).

$$\lg p_{\text{CO}} = 16.55 - 27404/T \quad (23)$$

$$\lg p_{\text{CO}} = 15.23 - 23433/T \quad (24)$$

$$\lg p_{\text{CO}} = 15.36 - 24528/T \quad (25)$$

$$\lg p_{\text{CO}} = 16.36 - 27506/T \quad (26)$$

The $\lg p_{\text{CO}}-1/T$ equilibrium diagram of metallic aluminum–CO system is plotted on the basis of Eqs. (22) to (26), and shown in Fig. 6. The curves represent the equilibrium conditions for the reactions, determining the areas of existence of various species:

1) The stability area of Al_4C_3 and CO_2 is on the right of the equilibrium curve of Reaction (6), and marked as “a”, where Reaction (6) mainly occurs.

2) The stability area of C and Al_2O_3 is between the equilibrium curves of Reactions (6) and (8), and marked as “b”, where Reaction (8) mainly occurs.

3) The stability area of C and $\text{Al}_4\text{O}_4\text{C}$ is between the equilibrium curves of Reactions (8) and (9), and marked as “c”, where Reaction (9) mainly occurs.

4) The stability area of Al_4C_3 and Al_2O_3 is between the equilibrium curves of Reactions (9) and (7), and marked as “d”, where Reaction (7) mainly occurs.

5) The stability area of $\text{Al}_4\text{O}_4\text{C}$ and Al_4C_3 is between the equilibrium curves of Reactions (7) and (10), and marked as “e”, where Reaction (10) mainly occurs.

6) The stability area of metallic aluminum and CO is on the left of the equilibrium curve of Reaction (10), and marked as “f”.

From Fig. 6, metallic aluminum and CO should react according to Reactions (6) and (8) to form $\text{Al}_4\text{C}_3+\text{CO}_2$ and $\text{Al}_2\text{O}_3+\text{C}$, respectively, at temperatures below 1250 K and CO partial pressures below 1000 Pa.

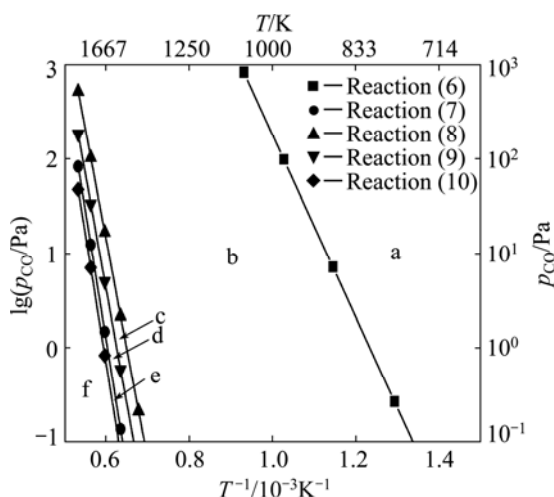


Fig. 6 Equilibrium diagram of metallic aluminum–CO system

The pressure at the exit of the vacuum furnace was maintained at 5–200 Pa in the experiment and CO accounted for about 98.5% of the off gas, and therefore the partial pressure of CO was approximated as 5–200 Pa. The partial pressure of CO in the condenser was higher than that at the exit, but could not reach 1000 Pa, and the temperature in the condenser was below about 1200 K, which means that metallic aluminum and CO in the condenser should react to form Al_4C_3 , CO_2 , Al_2O_3 and C, resulting in aluminum products containing Al_4C_3 , Al_2O_3 and C. This agrees with the experimental results, demonstrating that the reaction rate is very high and then the reaction system in vacuum is approximately in equilibrium. Consequently, the equilibrium diagram can be used to predict the reactions between metallic aluminum and CO in vacuum.

4 Conclusions

1) The required temperature for the disproportionation of CO decreases with decreasing

pressure in the range of 300–1900 K. The equilibrium temperatures are 917, 890 and 787 K, respectively, at the total pressure of 200, 100 and 5 Pa under condition that the disproportionation rate of CO is 1.5%.

2) The required temperature for each reaction of metallic aluminum and CO decreases with decreasing pressure in the range of 300–1900 K. The required temperatures for reactions of metallic aluminum with CO to form $\text{Al}_4\text{C}_3+\text{CO}_2$, $\text{Al}_2\text{O}_3+\text{C}$, $\text{Al}_4\text{O}_4\text{C}+\text{C}$, $\text{Al}_4\text{C}_3+\text{Al}_2\text{O}_3$, and $\text{Al}_4\text{O}_4\text{C}+\text{Al}_4\text{C}_3$ increase in turn.

3) The $\lg p_{\text{CO}}-1/T$ diagram of metallic aluminum–CO system was plotted, from which it can be deduced that metallic aluminum and CO react to form $\text{Al}_4\text{C}_3+\text{CO}_2$ and $\text{Al}_2\text{O}_3+\text{C}$ at temperatures below 1200 K and CO partial pressures below 1000 Pa, agreeing with the experimental results that the aluminum products contained Al_4C_3 , Al_2O_3 and C.

References

- [1] KUSIK C L, SYSKA A, MULLINS J, VEJINS V. Techno-economic assessment of a carbothermic alumina reduction process [C]//MACKEY T S, PRENGAMAN R D. Light Metals 1990. Warrendale: TMS, 1990: 1021–1034.
- [2] COCHRAN C N. Alternate smelting processes for aluminum part I [J]. Light Metal Age, 1987, 45(11–12): 15–20.
- [3] HALMANN M, FREI A, ATEINFELD A. Carbothermal reduction of alumina: Thermochemical equilibrium calculation and experimental investigation [J]. Energy, 2007, 32(12): 2420–2427.
- [4] BRUNO M J. Aluminum carbothermic technology [R]. Washington: U.S. Department of Energy Golden Field Office, 2004.
- [5] MURRAY J P. Aluminum production using high-temperature solar process heat [J]. Solar Energy, 1999, 66(2): 133–142.
- [6] WAI C M, HUTCHISON S G. A thermodynamic study of the carbothermic reduction of alumina in plasma [J]. Metallurgical and Materials Transactions B, 1990, 21(2): 406–408.
- [7] OTHMER D F. Method for producing aluminum metal directly from ore: USA, 3793003 [P]. 1974–02–19.
- [8] FENG Yue-bin, DAI Yong-nian, WANG Ping-yan. Research of the production and refining of aluminum by disproportion [J]. Light Metals, 2009(3): 12–15. (in Chinese)
- [9] WANG Ping-yan, LIU Mou-sheng, DAI Yong-nian. Vacuum metallurgy of Al from bauxite by carbothermic reduction-chlorination [J]. Chinese Journal of Vacuum Science and Technology, 2006, 26(5): 377–380. (in Chinese)
- [10] FENG Yue-bin, YU Qing-chun, YANG Bin, DAI Yong-nian. Extraction of aluminum from alumina by disproportionation process of AlCl in vacuum [J]. Transactions of Nonferrous Metals Society of China, 2013, 23(9): 2781–2785.
- [11] YUAN Hai-bin, FENG Yue-bin, XU Bao-qiang, YANG Bin, YU Qing-chun, DAI Yong-nian. Direct extraction of aluminum from alumina by carbothermic reaction-chlorination and possible mechanisms [J]. Chinese Journal of Vacuum Science and Technology, 2010, 30(3): 259–264. (in Chinese)
- [12] FENG Yue-bin, YANG Bin, DAI Yong-nian. Carbothermal reduction-chlorination-disproportionation of alumina in vacuum [J]. Transactions of Nonferrous Metals Society of China, 2012, 22(1): 215–221.
- [13] YU Wen-zhan, YANG Bin, ZHU Fu-long, JIANG Wen-long, YU Qin-chun, XU Bao-qiang. Investigation of chlorination process in

aluminum production by carbothermic–chlorination reduction of Al_2O_3 under vacuum [J]. Vacuum, 2012, 86(8): 1113–1117.

[14] ZHU Fu-long, YANG Bin, YUAN Hai-bin, YU Qing-chun, XU Bao-qiang, DAI Yong-nian. Silica behavior in the alumina carbothermic reduction-chlorination process [J]. JOM, 2011, 63(8): 119–122.

[15] YUAN Hai-bin, ZHU Fu-long, YU Qing-chun, LI Qiu-xia, XU Bao-qiang, YANG Bin, DAI Yong-nian. Effects of Fe_2O_3 , SiO_2 and TiO_2 on aluminum produced by alumina carbothermic reduction–chlorination process in vacuum [J]. The Chinese Journal of Nonferrous Metals, 2010, 20(9): 1836–1842. (in Chinese)

[16] DAI Yong-nian, YANG Bin. Vacuum metallurgy of nonferrous metal material [M]. Beijing: Metallurgical Industry Press, 2000: 278–345. (in Chinese)

[17] DAI Yong-nian, FENG Yue-bin, YANG Bin, YANG Bu-zheng, LIU Yong-cheng, XU Bao-qiang, LIU Da-chun, YU Qing-chun, MA Wen-hui, QING Bo. A kind of vacuum reaction furnace: China, 200920111773.1 [P]. 2009–08–06. (in Chinese)

真空 AlCl 歧化法生产铝的过程中 C 、 Al_4C_3 和 Al_2O_3 的形成热力学

冯月斌¹, 杨斌², 戴永年²

1. 昆明理工大学 理学院, 昆明 650500;
2. 昆明理工大学 治金与能源工程学院, 真空冶金国家工程实验室, 昆明 650093

摘要: 通过热力学分析研究了真空 AlCl 歧化法生产铝的过程中 C 、 Al_4C_3 和 Al_2O_3 的形成条件。结果表明, 形成这些杂质的反应, 即 CO 的歧化反应和金属铝与 CO 的反应, 所需的反应温度随着压力的降低而降低。金属铝– CO 体系的 $\lg p_{\text{CO}}-1/T$ 图与实验结果相符, 表明反应速率快, 该体系在真空下接近平衡, 该平衡图可以用来预测该体系在真空下可能的反应。

关键词: Al ; AlCl ; Al_2O_3 ; Al_4C_3 ; 歧化; 真空

(Edited by Hua YANG)